Research article

Jaka Petelin, Luka Černe, Jaka Mur, Vid Agrež, Jernej Jan Kočica, Joerg Schille, Udo Loeschner and Rok Petkovšek*

Pulse-on-demand laser operation from nanosecond to femtosecond pulses and its application for high-speed processing

https://doi.org/10.1515/aot-2021-0020
Received April 23, 2021; accepted June 25, 2021;
published online July 14, 2021

Abstract: In this manuscript we present a true pulse-on-demand laser design concept using two different approaches. First, we present a fiber master oscillator power amplifier (MOPA) based quasi-continuous wave (CW) laser, working at high modulation bandwidths, for generation of nanosecond pulses. Second, we present a hybrid chirped pulse amplification (CPA)-based laser, combining a chirped-pulse fiber amplifier and an additional solid-state amplifier, for generation of femtosecond pulses. The pulse-on-demand operation is achieved without an external optical modulator/shutter at high-average powers and flexible repetition rates up to 40 MHz, using two variants of the approach for near-constant gain in the amplifier chain. The idler and marker seed sources are combined in the amplifier stages and separated at the out using either wavelength-based separation or second harmonic generation (SHG)-generation-based separation. The nanosecond laser source is further applied to high throughput processing of thin film materials. The laser is combined with a resonant scanner, using the intrinsic pulse-on-demand operation to compensate the scanner's sinusoidal movement. We applied the setup to processing of indium tin oxide (ITO) and metallic films on flexible substrates.

Keywords: arbitrary repetition rate; fiber lasers; gain control; high speed processing; pulse-on-demand.

***Corresponding author: Rok Petkovšek**, Faculty of Mechanical Engineering, University of Ljubljana, Aškerčeva 6, SI-1000, Ljubljana, Slovenia, E-mail: rok.petkovsek@fs.uni-lj.si
Jaka Petelin, Luka Černe, Jaka Mur, Vid Agrež and Jernej Jan Kočica, Faculty of Mechanical Engineering, University of Ljubljana, Aškerčeva 6, SI-1000, Ljubljana, Slovenia
Joerg Schille and Udo Loeschner, University of Applied Sciences Mittweida, Laserinstitut Hochschule Mittweida, Schillerstraße 10, D-09648 Mittweida, Germany

1 Introduction

The ability to handle different processes with the same tool and to achieve high production throughputs is becoming more and more important for industrial applications. In order to satisfy these demands laser-based tools must be used in combination with high-speed scanning systems. Currently, the highest scanning speeds can be achieved with polygon [1] and resonant scanners [2] or with acousto-optic deflectors (AOD) [3, 4]. Although the later enables precise scanning with high resolution it is limited by the smaller working area and lower damage threshold compared to the first two. The use of high-speed scanning systems imposes stringent requirements also on the laser system itself. In order to achieve high processing resolution, the laser system must allow for rapid laser power modulation that is matched with the scanning speed. What is more, laser systems that are used in combination with polygon or resonant scanners must be able to operate at continuously variable repetition rates in order to generate arbitrary patterns on the workpiece [5]. The reason for this is that polygon scanners are limited to constant scanning speeds, which means that a laser with constant repetition rate would only generate equidistant structures on the workpiece. Similar issue arises with resonant scanners, where the speed of the laser beam on the workpiece sinusoidally changes due to the sinusoidal oscillation of the scanner mirror. Lasers that are compatible with both polygon and resonant scanners, that is that they are capable of generating arbitrary patterns on the workpiece, must therefore be able to generate laser pulses on demand [6].

There are several methods used that enable pulse-on-demand laser operation. One is a direct modulation of a continuous wave (CW) or fixed-repetition-rate lasers [7] with either acousto-optic modulators (AOM) or electro-optic modulators (EOM). The main limitation with direct modulation of the CW lasers is the low peak power of the laser pulses, which is not appropriate for all applications. Additionally, in order to achieve high modulation speeds

with AOM, tight focusing is required posing limitations on the laser power due to the damage threshold of the AOM. Similarly, in the case of EOM, the laser power is limited by the onset of thermal lensing caused by significant absorption in the EOM crystal.

Another approach is a direct modulation of high-power diode lasers, which enables relatively simple setups, but has a downfall of low beam quality compared to single mode or few mode laser systems. However, the high modulation bandwidth of these high-power diode lasers can be exploited if they are used as pump for gain switched lasers [8–12]. With gain switching technique a good control over pulse-generation dynamics can be achieved and therefore enabling pulse-on-demand operation with nearly single-mode beam quality. With this method laser pulses with several 10 s of ns can be achieved [13].

Although the above methods offer some outstanding flexibility, numerous new applications require ultrashort laser pulses. Therefore, different approaches to pulse-on-demand operation must be taken. One possible method arose with the development of the beam combination techniques. A precise phase control of the combined beams allows for pulse-on-demand operation by switching between constructive and deconstructive interference [14].

Other methods that offer ultrafast pulse-on-demand operation typically depend on some sort of gain control in the laser amplifiers. It is possible to directly modulate pump power [15], however, this method is often limited by the slow response times and in some cases must include advanced thermal management setups for pump wavelength stabilization [16]. A different approach uses additional idler light source which keeps the population inversion at constant level, between selected marker pulses, even in the case of continuous pumping of the amplifier [17–19]. In order to achieve pulse-on-demand operation, idler and marker light must be separated at the laser output, so that only marker pulses are sent to the workpiece. Two techniques for idler and marker separation are typically used. One is based on different polarizations or slightly different wavelengths of idler and marker pulses, so that they can be separated using a polarizing beam splitter or with an appropriate wavelength filter, respectively. The other method is to introduce long idler pulses or even CW idler light between short marker pulses. Due to different pulse durations, idler and marker pulses can be separated at the output via the second harmonic generation (SHG) [17, 20, 21].

High-speed high-throughput processing is the most relevant when a single laser pulse per spot is sufficient to achieve the desired material modification or ablation effect. Thin film materials, either conductive, semiconductive, or dielectric, are widely used in industrial and research applications, and fit to the mentioned criteria. Laser ablation and modification of indium tin oxide (ITO) layers has received widespread interest in recent years, with applications based on both nanosecond [22–26] and pico-/femtosecond [27–30] laser processing systems. Similarly, laser processing of metallic thin films is an active field of research, where either nanosecond [31–33] or pico-/femtosecond pulses [34–38] can cause the desired changes on the material. Thin film materials are mainly deposited on glass substrates, especially for basic research work, but work has been also done Cu films on a flexible polymer substrate [32] or ITO layers on polycarbonate plastics substrates [26], both relevant in industrial setting.

In this paper we present two laser sources, both using additional idler source to achieve gain control in the amplifiers, and both capable of producing pulses on demand with the ability to efficiently synchronize with the high-speed polygon and resonant scanners for covering different laser applications. Their capabilities are analyzed and the surface engineering application of thin film on flexible substrates using the described pulse-on-demand operation is presented.

2 Materials and methods

To ensure stable laser operation, the laser must be operated under constant conditions i.e., in either CW operation or at a fixed pulse repetition rate. In these cases, a steady state is achieved in a gain media. The problem arises when a pulse-on-demand operation is desired. With pulse-on-demand operation, pulse repetition rate is not constant which in return causes gain fluctuations in the laser amplifiers. A schematic of such fluctuations is presented in Figure 1, where we can see that without appropriate gain control, the amplitude of the laser pulses can vary significantly which is not desirable for most laser applications.

It can be seen from Figure 1(a), that if the interval between marker pulses increases, the population inversion and with that the gain in the amplifier also increases, causing high pulse amplitude in the first upcoming laser pulse, which can exceed the damage threshold of optical components in the laser systems. In order to avoid such detrimental effects, additional idler pulses are introduced instead of missing marker pulses, that prevent inversion population buildup and with that ensuring constant gain for all laser pulses Figure 1(b).

As it was already mentioned in the introduction, idler pulses must be separated from marker pulses at the laser output. There are several ways in which we can achieve this separation. In the following sections two methods will be presented in more detail. One is based on wavelength-based separation and the other implements a SHG unit that uses nonlinear optical processes, to filter out idler pulses from the pulse sequence.

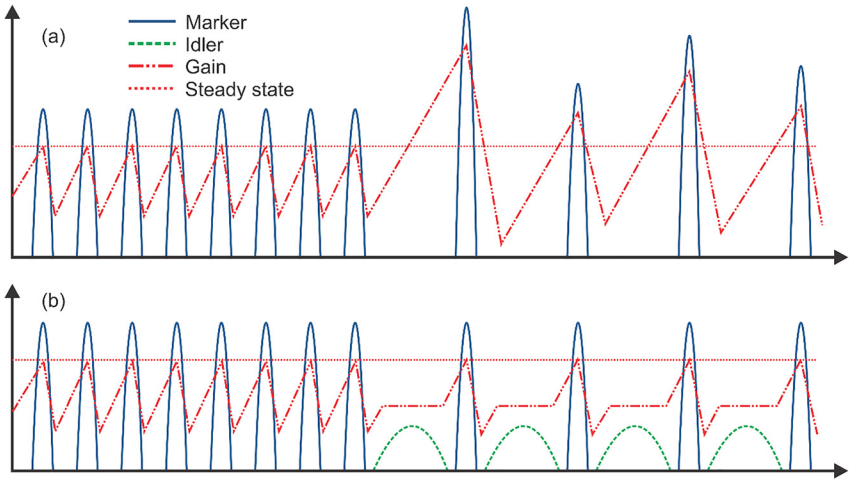

Figure 1: A schematic of pulse-to-pulse amplitude fluctuations. (a) When changing the laser operating conditions from a fixed repetition rate to a different repetition rate without additional gain control. With appropriate gain control i.e., with additional idler pulses (b), constant pulse energies can be achieved without transient fluctuations.

2.1 Wavelength-based separation

An experimental setup for pulse-on-demand operation based on a wavelength separation of idler and marker pulses is designed in a master oscillator power amplifier (MOPA) configuration and its schematic is presented in Figure 2. The MOPA design consists of two seed modules, one for idler and the other for marker pulses, which are then amplified in a single pass through two fiber amplifiers. The seed modules used are gain switched laser diodes operating at 1064 and 1060 nm generating marker and idler pulses, respectively. The length of marker and idler pulses can be varied from 20 ns up to CW operation. The Yb doped fiber amplifiers are pumped with 967 nm diode lasers, enabling 200 W of output laser power.

After the amplification stages, idler and marker pulses are separated with a volume Bragg grating (VBG) element, which reflects the light at marker wavelength and transmits the light at idler wavelength. The marker/idler pulse modulation bandwidth was 20–40 MHz.

2.2 SHG-based separation

Second harmonic generation is a nonlinear optical process and is therefore highly dependent on the laser pulse intensity. If the duration of the marker pulses is much shorter compared to idler pulses, the efficiency of the SHG process will be much higher for marker pulses compared to idler pulses. In this way we can efficiently eliminate idler pulses from the pulse sequence, sending only marker pulses to the workpiece. This method is therefore especially suitable for ultrashort marker pulses, that are combined with long (several ns) idler pulses as is the case in a here presented laser system.

The experimental setup of a femtosecond pulse-on-demand laser system is presented in Figure 3. It consists of a mode-locked fiber oscillator that generates picosecond marker pulses with 30 MHz repetition rate and with 1030 nm center wavelength. The pulses are then stretched to ~ps with a chirped fiber Bragg grating stretcher (CFBG). After first amplification stage, an acousto-optic modulator is used, to select only the desired marker pulses from the high repetition rate pulse train. Instead of missing marker pulses, additional idler pulses are introduced to the pulse train after the pulse picker. The idler pulse source is a gain switched laser diode, generating long pulses with ~30 ns duration. The combined pulse train is then amplified in two fiber amplification stages and one solid-state amplification stage. The solid-state amplification stage is needed to reduce the undesired nonlinear effects that occur due to high pulse intensities in the fiber amplifiers due to small core diameters of optical fibers [39]. The beam size in the solid-state amplifier is much larger compared to the fiber core size, which allows for additional pulse amplification with negligible nonlinear effects [40]. Fiber amplifiers are pumped with 976 nm laser diodes whereas the solid-state amplifier (Yb:YAG) is pumped with 969 nm laser diode.v

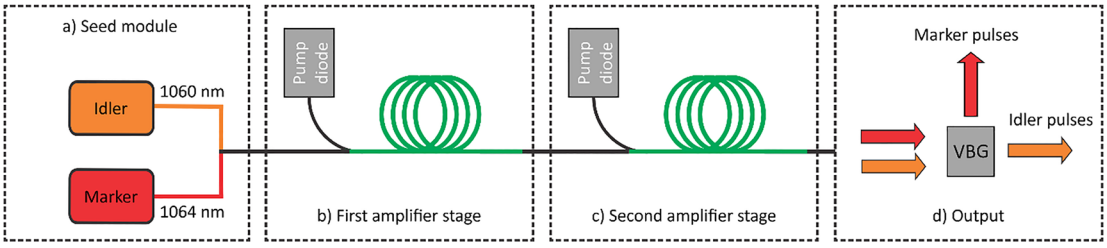

Figure 2: A schematic of an experimental setup for pulse-on-demand operation based on wavelength separation.
The system is designed in a MOPA configuration with two gain switched diodes used as a seed module (a). The wavelength of the idler seed diode was 1060 nm, and the wavelength of the marker seed diode was 1064 nm. The pulses were then amplified in two consecutive fiber amplifiers (b) and (c). After amplification, idler and marker pulses were separated with a VBG (d).

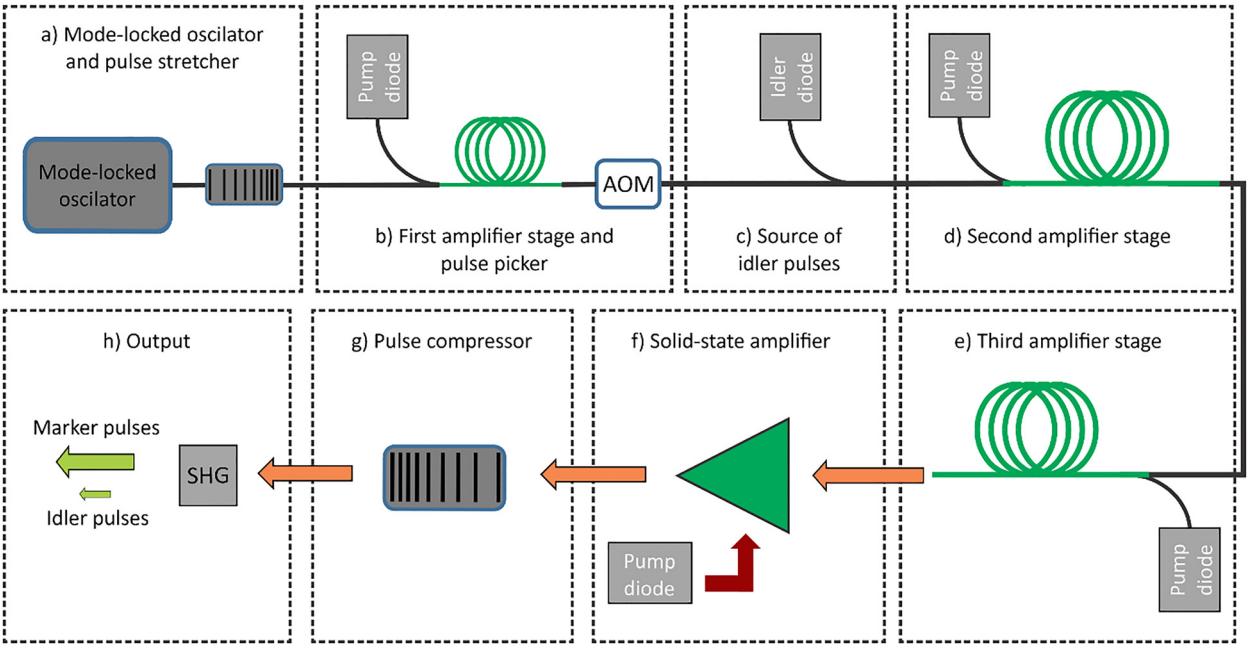

Figure 3: A schematic of a femtosecond pulse-on-demand laser system. The laser system comprises a mode-locked oscillator that generates ps laser pulses which are then stretched with a pulse stretcher (a). After the first amplification stage (b), the pulse picker which is an acousto-optic modulator picks the selected marker pulses from a high rep. rate pulse train coming from the oscillator. After the pulse picker, the idler pulses are introduced instead of missing marker pulses (c). The combined marker and idler pulses are then amplified in two fiber (d), (e), and one solid-state amplification stage (f). The marker pulses are then compressed with a pulse compressor (g) prior to second harmonic generation at the output (h).

After the amplification stages, the laser pulses are compressed with a grating compressor with 1700 l/mm in a Littrow configuration down to ~500 fs. The compressor efficiency is ~80%. Because of the narrow spectrum of the idler pulses, the pulse compression does not change their duration, so that they remain ~30 ns long. This large difference in pulse duration between marker and idler pulses results in 1:3000 contrast ratio in pulse energy after the SHG which translates to more than $1{:}10^8$ contrast ratio in pulse peak power.

2.3 Material processing setup

The MOPA-based laser was used for a material processing experimental setup including resonant scanner and AGC-PC driver electronics (model SC-30, Electro-Optical Products Corp.). The trigger out signal from the electronics board happened once per period of the resonant scanner, which was tuned to a resonant frequency around 3460 Hz. Each trigger was used as a starting point for each line scanned in *x*-direction, while in the perpendicular direction a mechanical stage was moving at a constant speed to ensure separation between the scanning lines. A precomposed sequence of laser pulses and pauses was sent to the laser at each trigger, ensuring the desired output laser pulses for the whole scanning line.

Deflection angles imposed by the scanner's position at the time of laser pulse incidence were imaged to the back aperture of a microscope objective by relay optics, to ensure laser beam positional stability at the entrance pupil. The laser beam pivoting point was translated from the resonant scanner' mirror surface to the microscope objective's back aperture (schematic in Figure 4(a)) We used two different objectives for laser beam focusing, a Thorlabs LMH-5X-1064 with 5× magnification and numerical aperture of 0.13 (effective focal length 40 mm), and an OptoSigma PAL-10-NIR with 10× magnification and numerical aperture of 0.3 (effective focal length 20 mm). Both objectives are optimized for laser beams at a 1064 nm wavelength. Given the input laser beam diameter the calculated laser spot sizes on material were 13 and 26 µm using the LMH-5× objective and 5 µm using the OptoSigma objective. Two different spot sizes through the same objective were a result of using different input beam diameters throughout the experiments. Laser pulse energy on material was up to 6 µJ and could be reached regardless of the pulse repetition rate or pulse sequence used.

The desired pulse position distribution on the material was recalculated into the requested pulse emission timings with respect to the resonant scanner's sinusoidal movement. The requested exact pulse timings were further recalculated on a discretized time domain to accommodate the 20 MHz repetition rate used in the experimental version of the laser source. In addition to the generation of best possible timings, we have also numerically simulated what kind of pulse distributions could be achieved with current state-of-the art lasers (2 MHz pulse-picker based pulse-on-demand operation) and compared those distributions on material for comparison within our experimental setup. The difference between timings of laser pulse emission and the corresponding position on the material is illustrated on graphs in Figure 4(b).

Materials used were metallic and transparent conductive oxide thin film materials. Sputter-coated aluminum film on glass substrate had a thickness of 40 nm, while the ITO on glass samples had 15–20 nm films. As the pinnacle of current industrial interest are

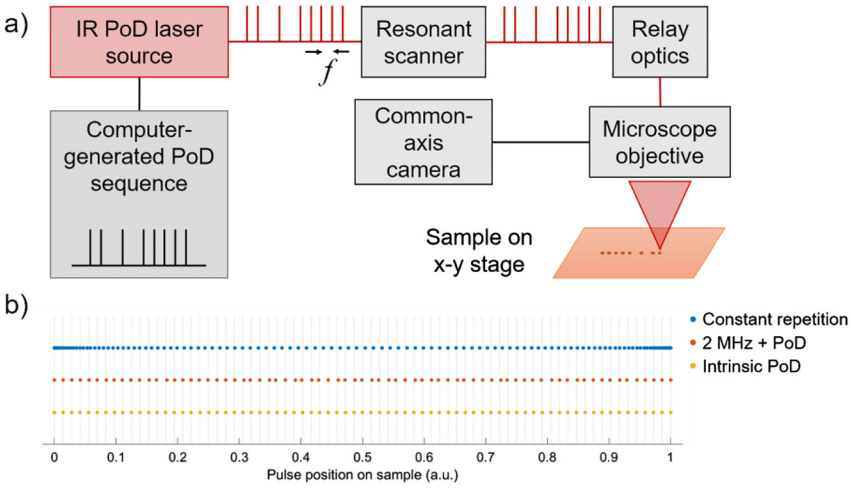

Figure 4: (a) Schematic illustration of the main the experimental system components. (b) The graph shows pulse positions on sample as functions of position along the scanning line for three different pulse distributions – at fixed repetition rate of 800 kHz (blue symbols), at fixed repetition rate of 2 MHz with external pulse picker for pulse-on-demand operation (red symbols), and with intrinsic pulse-on-demand at up to 20 MHz repetition rate (yellow symbols).

flexible materials, we have also obtained samples of Thorlabs OCF2520 ITO-coated PET sheets (total sheet thickness 0.2 mm), Teijin PFC100-D150 ITO-coated PC-sheets (total sheet thickness 0.1 mm), and PolyIC PolyTC Ag-coated PET sheet (total sheet thickness 0.05–0.075 mm). The substrate defines both the selective laser ablation process in terms of ablation thresholds as well as the adhesion of the thin film material.

The term intrinsic in Figure 4 refers to pulse on demand operation, where the desired pulse sequence is achieved with the laser itself. It is achieved by introducing additional idler pulses to replace the eliminated primary pulses from the desired pulse sequence. The idler pulses ensure constant inversion population of the gain media and therefore eliminate pulse to pulse fluctuations in the output pulse sequence.

3 Results and discussion

With the use of an additional idler source a stable pulse-on-demand operation was achieved with both presented laser systems. The achieved laser parameters and an example of their operation in pulse-on-demand regime are presented in the following sections, along with the example of an application with a resonant scanner and a pulse-on-demand operation of a laser.

3.1 Wavelength based separation

An example of pulse-on-demand sequence from a wavelength separation-based setup is shown in Figure 5. The results presented in this figure show a selected marker sequence on the workpiece, where the sequence is constructed from five marker pulses followed by the five missing pulses. On the figure only the peak powers of the pulses are shown as blue circles. From results presented we can see that almost no overshoot occurs when switching marker pulses on and off.

The achieved contrast between idler and marker pulses in the case presented in Figure 5 was 25 dB. The marker sequence duration could be varied from single pulse (20 ns) up to quasi-CW operation with marker modulation frequency

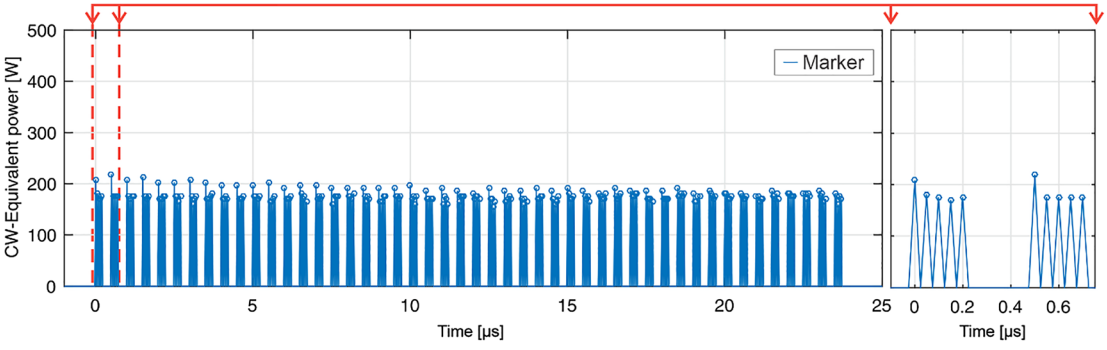

Figure 5: A selected pulse-on-demand sequence after wavelength separation of idler pulses from the marker pulses. A selected marker sequence consists of five marker pulses, followed by five missing marker pulses that were replaced by idler pulses. The figure shows only pulse peak powers that are presented with blue circles.

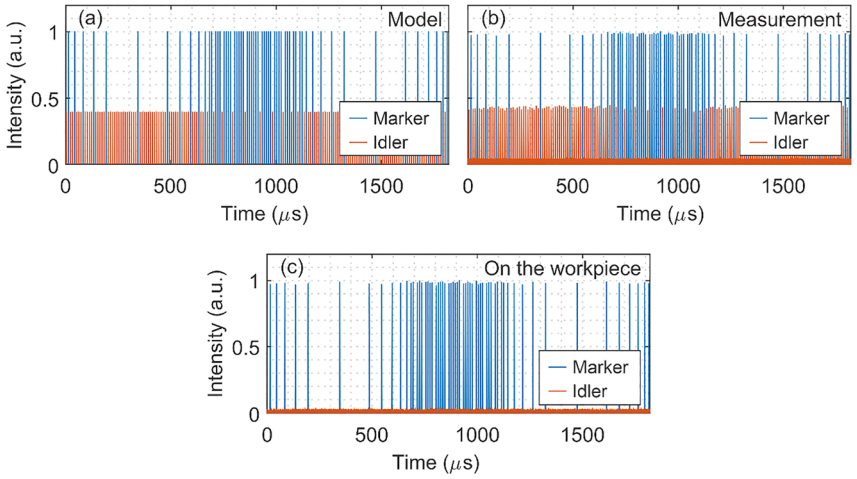

Figure 6: The figure shows simulated (a) and measured results (b) for a selected pulse-on-demand sequence both before (b) and after idler separation (c) with a SHG. The presented traces were measured with a photodiode and an oscilloscope. The amplitude of marker pulses is lower as they have longer pulse duration compared to the marker pulses. A presented sequence is constructed with varying number of marker pulses followed by varying number of idler pulses. Results published in [20].

of 40 MHz. The peak power of the marker pulses was ~200 W. With the presented laser system, a beam quality of $M^2 = 1.5$ was achieved.

3.2 SHG based separation

Similar results were obtained with the laser system that is based on a SHG separation of idler and marker pulses. A selected pulse-on-demand sequence obtained with this laser system is presented in Figure 6. The results show a comparison between the simulation results and measured results both before and after idler separation. The selected sequence consists of varying number of marker pulses followed by varying number of idler pulses, showing a true pulse-on-demand capability. From the results presented in Figure 6 we can see good agreement between the simulation and measured results, and what is more, we see, that the pulse energy is constant regardless of the interval between desired marker pulses.

For comparison with results presented in Figure 5 a different pulse-on-demand sequence was constructed also with a SHG separation-based system. The pulse-on-demand sequence shown in Figure 7 therefore consists of several marker sequences with varying duration. The marker pulses in each sequence were modulated with a 2 MHz repetition rate. Between the marker sequences idler pulses were introduced as gain control and were filtered at the output with a SHG. From the presented figure we can see that an arbitrary duration of marker sequence can be achieved with arbitrary interval between the desired marker sequences without any transient effects when switching between marker and idler pulses.

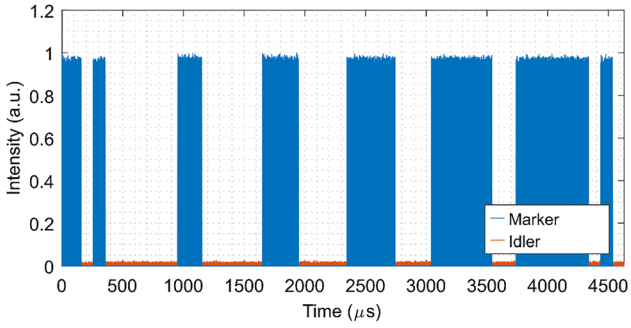

Figure 7: A measured pulse-on-demand sequence after SHG in a hybrid laser system. Results published in [20].

With the SHG method of marker and idler separation a contrast of 35 dB in pulse energies was achieved which corresponds to a contrast of 80 dB in pulse peak power between idler and marker pulses. This high peak power contrast is a consequence of large difference between idler and marker pulse durations, where the first are several 10 s of ns long and the second are compressed to ~500 fs.

The presented laser system enabled us to achieve pulse-on-demand operation with ultrashort marker pulses with 450 fs duration and with up to 300 μJ pulse energy. The measured autocorrelation trace of the marker pulses is shown in Figure 8. From the results in Figure 8 we can see that the measured autocorrelation trace is in good agreement with the theoretical autocorrelation trace that correspond to ideal Sech^2 pulses. There is almost no pedestal or sidelobes present in the autocorrelation trace, indicating that all pulse energy is concentrated in a short time interval around the maximum. The output laser beam from this hybrid laser operating at pulse-on-demand had a M^2 of 1.4.

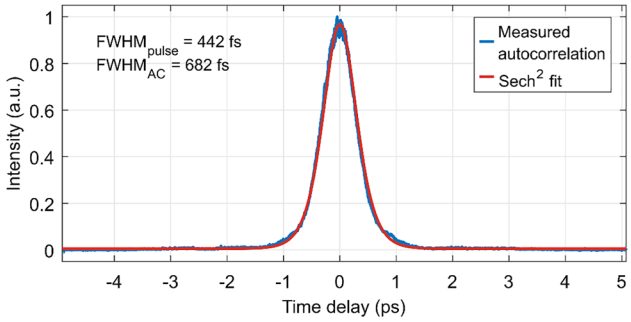

Figure 8: Measured autocorrelation trace of marker pulses with 300 µJ energy and comparison with theoretical autocorrelation from ideal Sech^2 pulses. Results published in [20].

3.3 Thin film processing results

Two laser operation modes were chosen for comparison to our variable repetition rate laser source, and to highlight the advantages of a native pulse-on-demand mode for controlled material processing. At a constant repetition rate of 800 kHz, evenly spaced craters at an interval of 45 µm were manufactured at the middle of the scanning range, while exhibiting highly accumulated laser pulses at the beginning and end. The second option, a simulated operation at 2 MHz with the pulse picker at output, irregularities in the crater pattern where observed (varying distance between neighboring craters), in line with the calculations. Using the intrinsic pulse-on-demand capabilities at 20 MHz, the achieved positioning accuracy was 3 µm or better throughout the scanner's range, while the scanning speed on material was up to 60 m/s and the average scan speed of around 21 m/s. We used the focusing setting corresponding to the calculated beam diameter of 13 µm on material in this case (see Figure 9).

We demonstrated the capability to use a constant scanning regime combined with intrinsic pulse-on-demand laser operation to create arbitrary patterns on thin film materials. Arbitrary patterns are composed of continuous lines of arbitrary lengths and arbitrary pauses in between, i.e. are based on the ability to either separate the consequent pulses for as long as necessary or create sequences of pulses at continuously varying repetition rates. ITO on glass was used as a proof of concept – to check whether appropriate ablation conditions can be achieved under the given focusing conditions. Single craters were successfully structured with the available pulse fluence, but the continuous line proved to be an issue with the ITO residue left on the substrate after the process of laser ablation, regardless of the laser fluence used. IR nanosecond laser pulses are only weakly absorbed in the glass substrate, therefore no damage to the substrate was expected and it was not observed either. Additional research is needed to investigate the observed phenomena and compare the results with other literature. Some related work shows that use of significantly shorter laser pulses (10 ps) is beneficial under such circumstances, while showing rather similar results to ours when using ps pulses. The two other materials processed were thin film materials on flexible substrates. A successful creation of various patterns was observed on both, ITO on PET and Ag on PET materials (Figure 10(b) and (d)). Contrary to the aforementioned experiments, the formation of a continuous line in ITO on PET was created without residue. Rougher line edges in Ag on PET point to thin film materials' weaker adhesion to the substrate compared to the ITO film on glass, and similar conclusion may be true for ITO on PET. The weaker adhesion is confirmed by the AFM imaging of the ITO crater in Figure 10(c), where a part of the ITO layer is hanging over the crater's middle left side edge. A highly localized process of peeling or laser-induced lift-off, either probably catalyzed by the weaker adhesion, also induced the rougher line edges in the Ag on PET material, as seen in bottom of Figure 10(d).

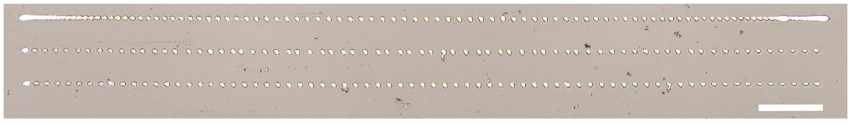

Figure 9: Experimental realization of three different laser modes, shown from top to bottom as following: Constant 800 kHz pulse repetition rate, 2 MHz pulse repetition rate with pulse picker emission control, and full pulse-on-demand at 20 MHz. We have observed small deviations from circular crater shapes, which are mostly the result of the initial beam profile, quality, and astigmatism. Scale bar equals to 200 µm. Result published in [5].

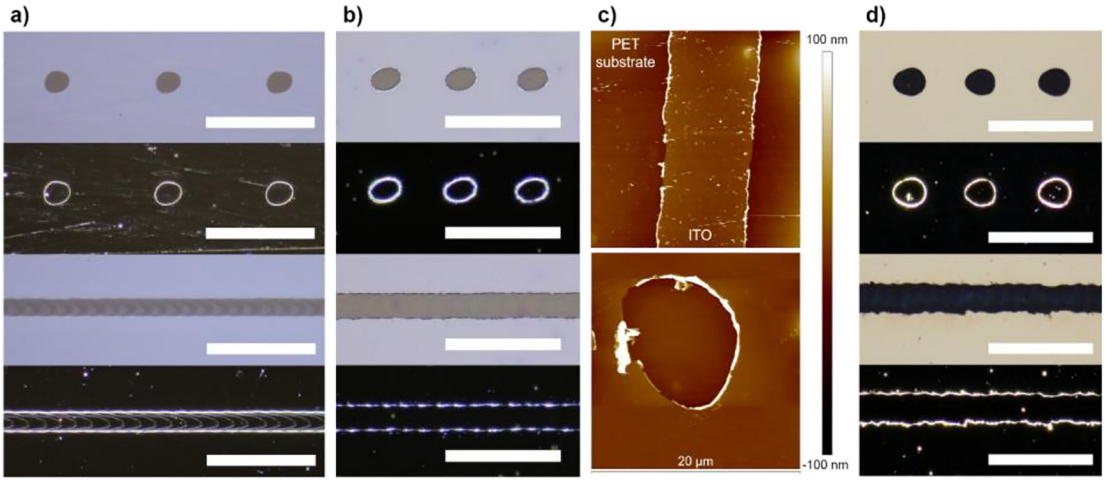

Figure 10: (a) Bright field (first and third image) and dark field (second and fourth image) views of structured ITO on glass – ITO layer not completely removed in lines. (b) Structured Thorlabs OCF2520 ITO-coated PET sheet – selective ablation of ITO thin film observed with negligible damage to the substrate. (c) AFM imaging of a conductive line and a single crater in ITO. (d) Structured PolyIC PolyTC Ag-coated PET sheet – selective ablation of Ag thin film with small effects on the substrate. Scale bars equal to 50 µm.
Result published in [5].

4 Conclusion

True pulse-on-demand operation, intrinsically achieved with the laser design, must result in equal pulse energies of output pulses, regardless of the emission timing. Transient pulse dynamics must therefore be carefully taken care of, typically with a chosen gain control mechanism. Additional complexity must be considered with a hybrid laser design, i.e. when combining fiber amplifier with a solid-state amplifier, because different gain spectra are combined in a single end effect.

In this work, we presented two approaches to achieve pulse-on-demand sequences with minimal transient pulse energy dynamics, regardless of the pulse frequency variability. The method of gain control was to insert idler pulses instead of primary seed pulses when the output is not needed, to achieve a stable amplifier chain gain, and separate the two pulse streams at the laser output. Nanosecond pulses were wavelength separated, while femtosecond pulses were separated by their duration in combination with SHG efficiency difference due to peak power.

To test the custom-made laser source pulse-on-demand capabilities on a material processing application, we have developed an experimental setup that combines the laser with an ultrafast resonant scanner to achieve ultrafast surface modification. The pulse-on-demand capabilities, approximately an order of magnitude faster compared to the industrial-standard pulse picker solutions, were the enabling factor in achieving the structuring speed and precision demonstrated on the application.

We have demonstrated selective thin film surface structuring on both ITO and metallic films on flexible substrates, while an ITO layer on glass was fully achieved in processing of single spots. The thin film material response to nanosecond laser pulses was well confined to the center of the laser beam, exhibiting little influence on the surrounding material and/or on the underlying substrate, regardless of the material type used. This points to the high-frequency high-power nanosecond source being a highly suitable laser choice for the application, presenting a cost-effective option, with possible further improvement in both the average output power and repetition rate.

Further research and experimental work is planned on characterization of the femtosecond laser source on high speed material processing applications, aimed at demanding applications combining improved precision, and process control while scaling down the feature size towards high speed microprocessing.

Author contributions: All the authors have accepted responsibility for the entire content of this submitted manuscript and approved submission.
Research funding: This work was funded by Slovenian Research Agency (P2-0270) (L2-9240).
Conflict of interest statement: The authors declare no conflicts of interest regarding this article.

References

[1] R. De Loor, "Polygon scanner system for ultra short pulsed laser micro-machining applications," *Phys. Procedia*, vol. 41, pp. 544–551, 2013.

[2] F. Harth, M. C. Piontek, T. Herrmann, and J. A. L'huillier, "Ultra high-speed micromachining of transparent materials using high PRF ultrafast lasers and new resonant scanning systems," in *Proc. SPIE 9736, Laser-based Micro- and Nanoprocessing X*, vol. 97360N, San Francisco, CA, USA, SPIE LASE, 2016, p. 97360N.

[3] J. Mur, B. Kavčič, and I. Poberaj, "Fast and precise Laguerre–Gaussian beam steering with acousto-optic deflectors," *Appl. Opt.*, vol. 52, no. 26, pp. 6506–6511, 2013.

[4] J. Mur, B. Podobnik, and I. Poberaj, "Laser beam steering approaches for microstructuring of copper layers," *Opt. Laser. Technol.*, vol. 88, pp. 140–146, 2017.

[5] J. Mur, J. Petelin, J. Schille, U. Loeschner, and R. Petkovšek, "Ultra-fast laser-based surface engineering of conductive thin films," *Appl. Surf. Sci.*, vol. 509, p. 144911, 2019.

[6] R. Petkovšek, V. Agrež, J. Petelin, L. Černe, U. Bünting, and B. Podobnik, "Pulses on demand in fibre and hybrid lasers," *SV-JME*, vol. 65, no. 11–12, pp. 680–689, 2019.

[7] M. Šajn, J. Petelin, V. Agrež, M. Vidmar, and R. Petkovšek, "DFB diode seeded low repetition rate fiber laser system operating in burst mode," *Opt. Laser. Technol.*, vol. 88, pp. 99–103, 2017.

[8] R. Petkovšek, V. Agrež, F. Bammer, P. Jakopič, and B. Lenardič, "Experimental and theoretical study of gain switched Yb-doped fiber laser," in *Proc. SPIE 8601, Fiber Lasers X: Technology, Systems, and Applications*, 2013, p. 860128.

[9] V. Agrež and R. Petkovšek, "Gain-switched Yb-doped fiber laser for microprocessing," *Appl. Opt.*, vol. 52, no. 13, pp. 3066–3072, 2013.

[10] J. Yang, Y. Tang, and J. Xu, "Development and applications of gain-switched fiber lasers," *Photonics Res.*, vol. 1, no. 1, pp. 52–57, 2013.

[11] V. Agrež and R. Petkovšek, "Gain switch laser based on micro-structured Yb-doped active fiber," *Opt. Express*, vol. 22, no. 5, pp. 5558–5563, 2014.

[12] R. Petkovšek, V. Agrež, D. Sangla, J. Saby, R. B. Picard, and F. Salin, "Gain-switched ytterbium-doped rod-type fiber laser," *Laser Phys. Lett.*, vol. 11, no. 10, p. 105808, 2014.

[13] R. Petkovšek and V. Agrež, "Single stage Yb-doped fiber laser based on gain switching with short pulse duration," *Opt. Express*, vol. 22, no. 2, pp. 1366–1371, 2014.

[14] S. Breitkopf, A. Klenke, T. Gottschall, et al, "GHz-bursts and ultrafast external modulation of femtosecond fiber lasers with kW average power levels," in *2019 Conference on Lasers and Electro-Optics Europe and European Quantum Electronics Conference*, p. cm_7_2, OSA Technical Digest, San Jose, CA, USA, 2019. [Online]. Available at: https://www.osapublishing.org/abstract.cfm?uri=CLEO_Europe-2019-cm_7_2 [accessed Feb. 11, 2020].

[15] K. Motoshima, L. M. Leba, D. N. Chen, M. M. Downs, T. Li, and E. Desurvire, "Dynamic compensation of transient gain saturation in erbium-doped fiber amplifiers by pump feedback control," *IEEE Photonics Technol. Lett.*, vol. 5, no. 12, pp. 1423–1426, 1993.

[16] V. Novak, B. Podobnik, J. Možina, and R. Petkovšek, "Analysis of the thermal management system for a pump laser," *Appl. Therm. Eng.*, vol. 57, no. 1–2, pp. 99–106, 2013.

[17] F. Harth, T. Herrmann, and J. A. L'huillier, "High power ultrafast laser with highly dynamic repetition rate and constant pulse energy from single pulse to 10 MHz," in *Proc. SPIE 10896, Solid State Lasers XXVIII: Technology and Devices*, vol. 108960H, San Francisco, CA, USA, SPIE LASE, 2019, p. 108960H.

[18] R. Petkovšek, V. Novak, and V. Agrež, "High power fiber MOPA based QCW laser delivering pulses with arbitrary duration on demand at high modulation bandwidth," *Opt. Express*, vol. 23, no. 26, pp. 33150–33156, 2015.

[19] R. Petkovšek, V. Novak, and V. Agrež, "Fiber laser for high speed laser transfer printing," in *Proc. SPIE 10254, XXI International Symposium on High Power Laser Systems and Applications 2016*, 2017, vol. 0254, p. 1025403.

[20] L. Černe, J. Petelin, and R. Petkovšek, "Femtosecond CPA hybrid laser system with pulse-on-demand operation," *Opt. Express*, vol. 28, no. 6, pp. 7875–7888, 2020.

[21] U. Quentin, F. Kanal, A. Budnicki, et al, "TruMicro 2000: next-generation flexible ultrashort pulse fiber lasers for scientific and industrial applications," in *Proc. SPIE 10897, Fiber Lasers XVI: Technology and Systems*, vol. 108971M, San Francisco, CA, USA, SPIE LASE, 2019.

[22] O. Yavas and M. Takai, "High-speed maskless laser patterning of indium tin oxide thin films," *Appl. Phys. Lett.*, vol. 73, no. 18, pp. 2558–2560, 1998.

[23] C. Molpeceres, S. Lauzurica, J. L. Ocaña, J. J. Gandía, L. Urbina, and J. Cárabe, "Microprocessing of ITO and a-Si thin films using ns laser sources," *J. Micromech. Microeng.*, vol. 15, no. 6, pp. 1271–1278, 2005.

[24] M. Y. Xu, J. Li, L. D. Lilge, and P. R. Herman, "F2-laser patterning of indium tin oxide (ITO) thin film on glass substrate," *Appl. Phys. A*, vol. 85, no. 1, pp. 7–10, 2006.

[25] Z. H. Li, E. S. Cho, and S. J. Kwon, "A new laser direct etching method of indium tin oxide electrode for application to alternative current plasma display panel," *Appl. Surf. Sci.*, vol. 255, no. 24, pp. 9843–9846, 2009.

[26] M.-F. Chen, W.-T. Hsiao, Y.-S. Ho, S.-F. Tseng, and Y.-P. Chen, "Laser patterning with beam shaping on indium tin oxide thin films of glass/plastic substrate," *Thin Solid Films*, vol. 518, no. 4, pp. 1072–1078, 2009.

[27] N. Farid, H. Chan, D. Milne, A. Brunton, and G. M. O'Connor, "Stress assisted selective ablation of ITO thin film by picosecond laser," *Appl. Surf. Sci.*, vol. 427, pp. 499–504, 2018.

[28] D. Ashkenasi, G. Müller, A. Rosenfeld, et al, "Fundamentals and advantages of ultrafast micro-structuring of transparent materials," *Appl. Phys. A*, vol. 77, no. 2, pp. 223–228, 2003.

[29] G. Raciukaitis, M. Brikas, M. Gedvilas, and G. Darcianovas, "Patterning of ITO on glass with picosecond lasers for oleds," *ICALEO*, vol. 2006, no. 1, p. M304, 2006.

[30] C. W. Cheng, I. M. Lee, and J. S. Chen, "Femtosecond laser processing of indium-tin-oxide thin films," *Opt. Laser. Eng.*, vol. 69, pp. 1–6, 2015.

[31] E. Matthias, M. Reichling, J. Siegel, et al, "The influence of thermal diffusion on laser ablation of metal films," *Appl. Phys. A*, vol. 58, no. 2, pp. 129–136, 1994.
[32] D. Paeng, J.-H. Yoo, J. Yeo, et al, "Low-cost facile fabrication of flexible transparent copper electrodes by nanosecond laser ablation," *Adv. Mater.*, vol. 27, no. 17, pp. 2762–2767, 2015.
[33] P. Lorenz, M. Klöppel, T. Smausz, et al, "Dynamics of the laser-induced nanostructuring of thin metal layers: experiment and theory," *Mater. Res. Express*, vol. 2, no. 2, p. 026501, 2015.
[34] Z. Wang, S. Kuk, W. M. Kim, J. Jeong, and D. J. Hwang, "Picosecond laser scribing of bilayer molybdenum thin films on flexible polyimide substrate," *Appl. Surf. Sci.*, vol. 493, pp. 320–330, 2019.
[35] G. Heise, M. Domke, J. Konrad, S. Sarrach, J. Sotrop, and H. P. Huber, "Laser lift-off initiated by direct induced ablation of different metal thin films with ultra-short laser pulses," *J. Phys. D Appl. Phys.*, vol. 45, no. 31, p. 315303, 2012.
[36] S. Xiao, B. Schöps, and A. Ostendorf, "Selective ablation of thin films by ultrashort laser pulses," *Phys. Procedia*, vol. 39, pp. 594–602, 2012.
[37] D. J. Joe, S. Kim, J. H. Park, et al, "Laser–material interactions for flexible applications," *Adv. Mater.*, vol. 29, no. 26, p. 1606586, 2017.
[38] S. I. Kudryashov and A. A. Ionin, "Multi-scale fluence-dependent dynamics of front-side femtosecond laser heating, melting and ablation of thin supported aluminum film," *Int. J. Heat Mass Tran.*, vol. 99, pp. 383–390, 2016.
[39] L. Černe, J. Novak, V. Agrež, and R. Petkovšek, "Optimization of a supercontinuum source based on tapered ordinary fibers," *Laser Phys.*, vol. 29, no. 2, p. 025103, 2019.
[40] L. Černe, P. Šušnjar, and R. Petkovšek, "Compensation of optical nonlinearities in a femtosecond laser system in a broad operation regime," *Opt. Laser. Technol.*, vol. 135, p. 106706, 2021.